Longitudinal Phase Space Reconstruction

Peter Denton

Lee Teng Summer Internship Program at Fermilab
with Tanaji Sen

August 7, 2009

Abstract

Standard rf cavities employ a sinusoidal wave to accelerate many bunches. The Recycler at Fermilab has used a barrier bucket to contain one bunch. This requires a new look at the longitudinal phase space and modifications to the normal method of reconstructing the two dimensional phase space from one dimensional line shapes. Finally comparisons to predictions from the Vlasov equation can assess the accuracy of each method.

Overview

Project Overview

The focus of this project was to analyze and reconstruct the longitudinal phase space in the Recycler with its barrier bucket rf wave. To accomplish this, I first did some simple modeling of particles in a regular sine wave and a barrier bucket to get a feel for how exactly they are different. This also allowed me to look at how the tune varied in one versus the other. Next, I needed real data to run, so I took line shapes of the Main Injector and the Recycler. Next, I worked through the CERN tomography code and analyzed reconstructed the phase space of the Main Injector. Finally, I adjusted the code to work with the Recycler. I also wrote some scripts for the Vlasov program to display the current phase space as the bunch goes around the accelerator.

Tomography

It is not possible to directly measure the two dimensional longitudinal phase space of a beam, and so line shapes of the same bunch(es) (see Figure 2) are taken which are then used to reconstruct the full phase space. As time progresses, particles rotate in phase space. By taking one dimensional line shape snapshots as they rotate as shown in the mountain range plot (Figure 1) it is possible to use these to recreate the original phase space from the one dimensional projections. As a phase space model is built up, it is then back projected to the original line shapes and compared. Iterating gives a good approximation of the original phase space. In addition, particle tracking is employed. That is, a number of particles are launched through the phase space and compared to the original line shapes. This hybrid algorithm produces very accurate results.

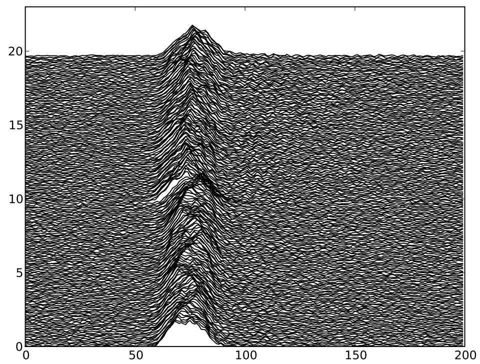

(a) The line shapes of a bunch in the Main Injector across each trace in a mountain range plot.

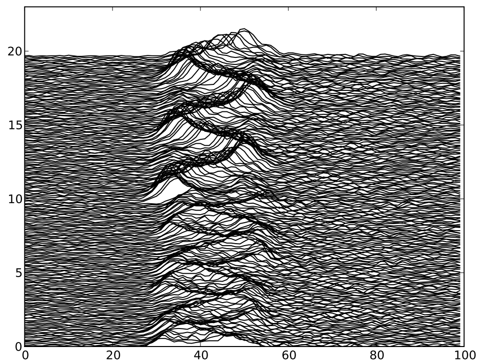

(b) Main Injector line shape for a different bunch with more moments

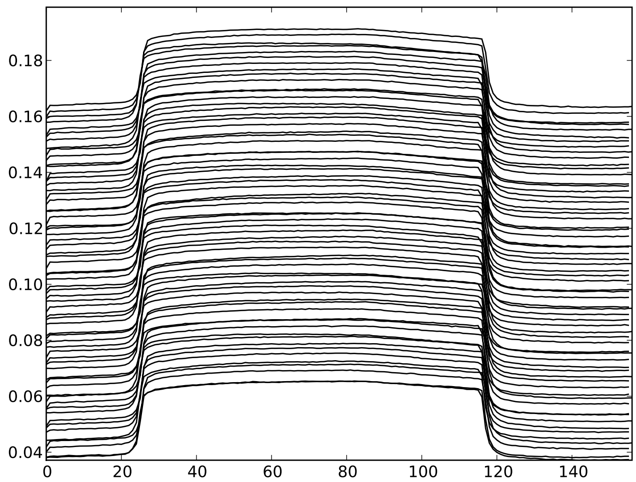

(c) The line shapes of a bunch in the Recycler across each trace in a mountain range plot.

Figure 1: Line shapes in the Main Injector and Recycler.

Parameter	Main Injector	Recycler
Energy (GeV)	120	8.9
Radius (m)	528.3	528.3
Magnetic field (T)	1.72	0.145
Bending radius (m)	232.55	203.2
γ_{tr}	21.62	19.97
$\lvert\eta\rvert$	0.00208	0.0086
V_{rf}	1.1 MV	1.8 kV
h	588	1

Table 1: The parameters of the Main Injector and the Recycler during data acquisition.

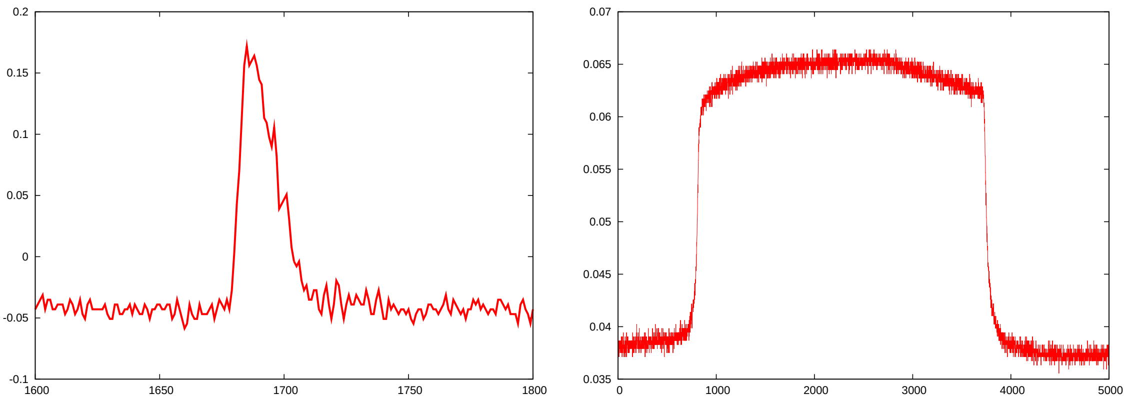

(a) Main Injector line shape

(b) Recycler line shape

Figure 2: The line shapes of the Main Injector and the Recycler. The Recycler line shape is roughly square with hard edges as opposed to a more typical shape similar to a Gaussian as seen in the Main Injector.

Accelerator Parameters

Data was taken across two accelerators, the Main Injector and the Recycler, which both reside in the same tunnel at Fermilab. The data, as it was taken, can be seen in Figure 2. This is all of the data that is used to reconstruct the phase space. Their conditions at data acquisition are outlined in Table 1.

Path Modeling

My first project was to write code to model paths in an ideal sine wave rf bucket using some parameters from the Tevatron and the recursive algorithm[2] for the energy and the phase as a function of turns.

$$\begin{cases} \Delta E_{n+1} & = \Delta E_n + eV(\sin\phi_n - \sin\phi_s) \\ \phi_{n+1} & = \phi_n + \frac{2\pi h\eta}{\beta^2 E}\Delta E_{n+1}. \end{cases} \tag{1}$$

In addition, I solved the Hamiltonian for the separatrix,

$$H = \frac{1}{2}\frac{h\eta}{\beta^2 E}(\Delta E)^2 + \frac{eV}{2\pi}[\cos\phi - \cos\phi_s + (\phi - \phi_s)\sin\phi_s] \tag{2}$$

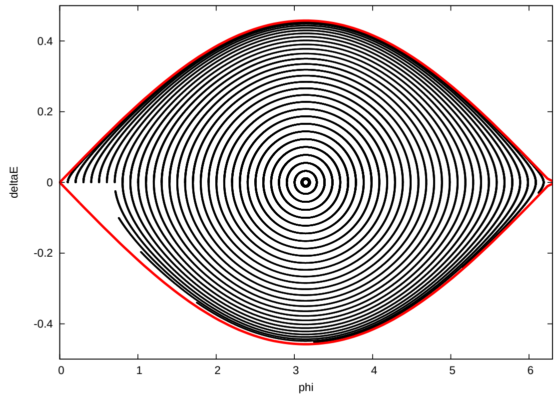

Figure 3: In the phase space diagram for a sine rf waveform, the outer particles move more slowly since the period increases with amplitude. The inner particles move nearly as ellipses which are increasingly deformed as amplitude is increased.

$$(\Delta E)^2 = \frac{eV\beta^2 E}{\pi h \eta}(1 - \cos\phi) \tag{3}$$

which is shown with several particle traces in Figure 3. Note that the period increases as a function of radius. Next, I repeated the process for a barrier bucket as shown in Figure 4. The bucket, in phase space, is given by

$$\begin{cases} (\Delta E)^2 = \frac{eV\beta^2 E}{\pi h \eta}\phi & \text{for } 0 < \phi < 2\pi\frac{T_1}{2T_1+T_2} \\ (\Delta E)^2 = \frac{eV\beta^2 E}{\pi h \eta}\frac{1}{2} & \text{for } 2\pi\frac{T_1}{2T_1+T_2} < \phi < 2\pi\frac{T_1+T_2}{2T_1+T_2} \\ (\Delta E)^2 = \frac{eV\beta^2 E}{\pi h \eta}(2\pi - \phi) & \text{for } 2\pi\frac{T_1+T_2}{2T_1+T_2} < \phi < 2\pi. \end{cases} \tag{4}$$

as seen in Figure 5. Modifying a Fast Fourier Transform [3] code I found the tune, Figure 6 as a function of the frequency for both the sine and barrier buckets. The tune of the barrier rf wave has a rather different shape as shown in Figure 7. Focusing on the rising part of the wave, and varying the ratio of $T1$ to $T2$ where $T1$ is the width of each pulse and $T2$ is the width of the empty area in between, we see (Figure 8) that as the ratio increases across $^1/_4$, we see that the tune obtains a local maximum which could lead to instabilities.

Data Collection

With Dr. Bhat's assistance, I became familiar collecting data from the main control room. I took data from the Recycler with a barrier rf wave, as well as the Main Injector with a typical sine rf wave for comparison and to use to become familiar with the tomography code. The Main Injector data was taken at 120 GeV with 84 bunches circling and the Recycler data was taken at 8 GeV immediately before and immediately after injection. Next I tracked down the source code for the program used to write the code in order to write it from binary to ascii.

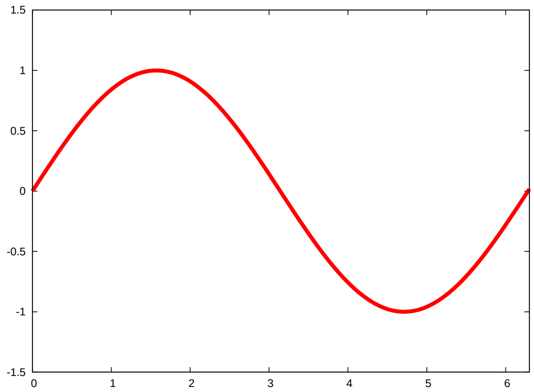

(a) The sine wave form.

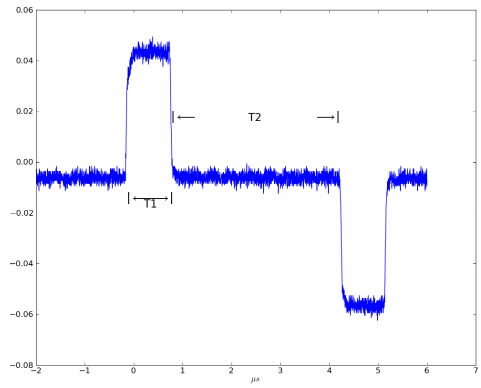

(b) The barrier bucket wave form. $T1$ is the width of the pulses while $T2$ is the width between the pulses of 0 voltage.

Figure 4: The wave forms in the Main Injector and the Recycler

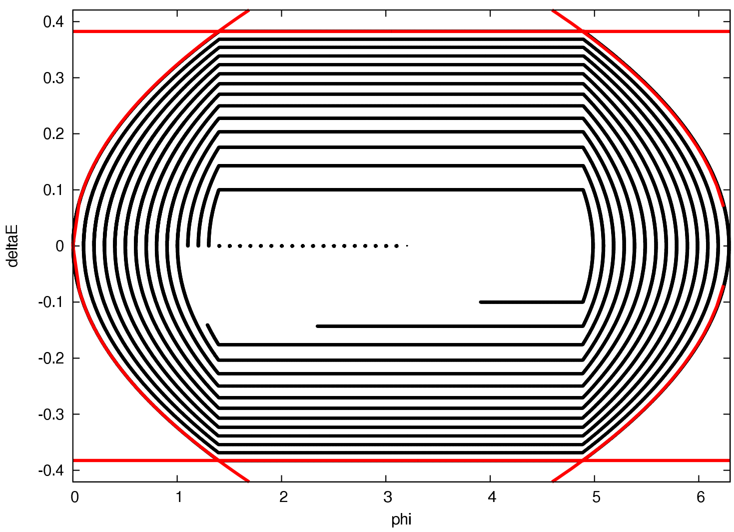

Figure 5: In the phase space diagram for a barrier barrier rf waveform, the outer particles move more quickly through parabolas and then lines of constant energy. Moreover, those in the middle are not kicked at all, and thus have no tune (see Figure 7).

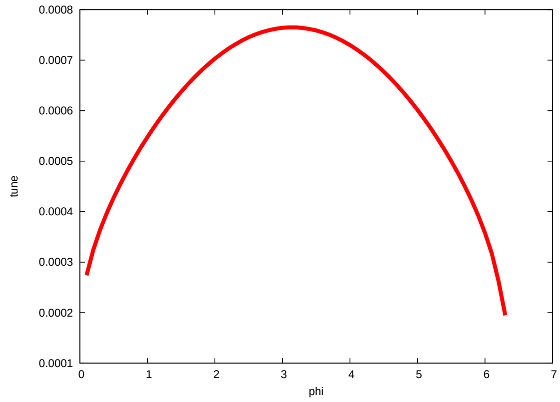

Figure 6: The tune of particles in a sine rf bucket as a function of phi. Note that as particles move toward the center, their tune and correspondingly their synchrotron frequency increases.

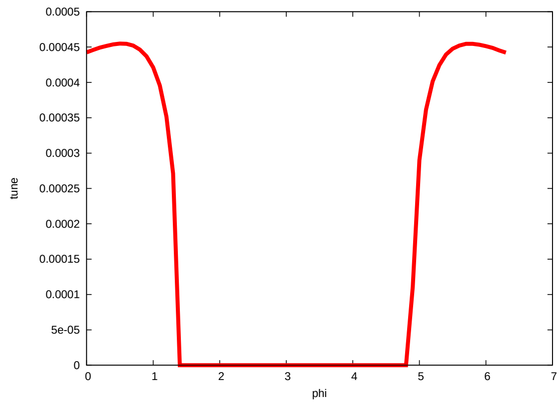

Figure 7: The tune of particles in a barrier rf bucket as a function of phi. Note that the tune is 0 for particles with $\Delta E = 0$ and phase within the middle of the barriers.

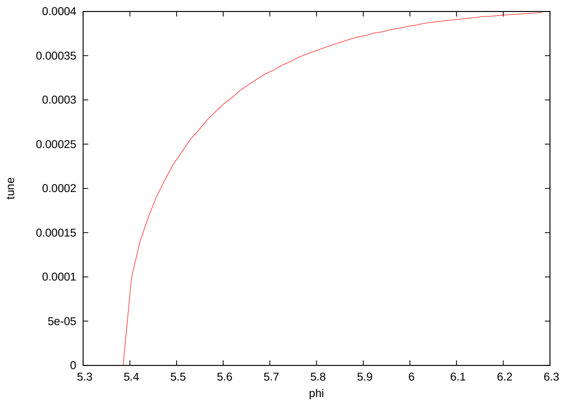

(a) ${}^{T1}/_{T2} = 0.20$

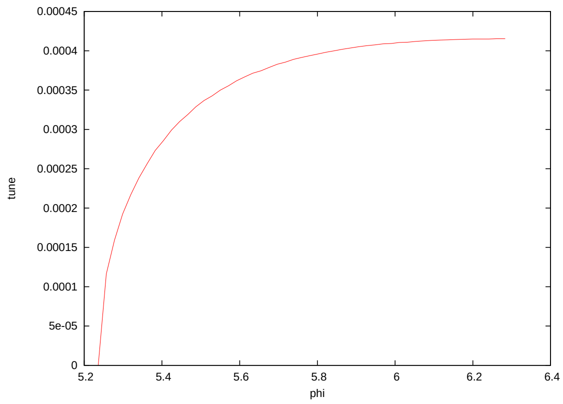

(b) ${}^{T1}/_{T2} = 0.25$

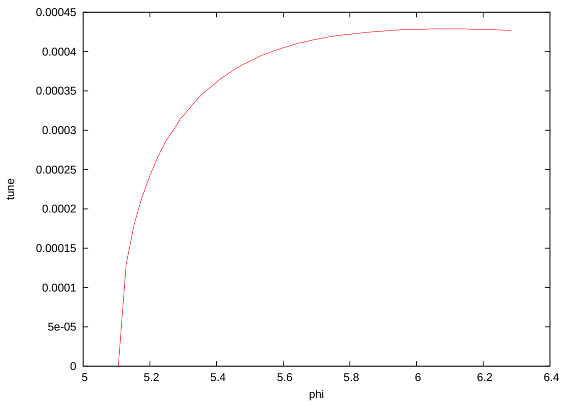

(c) ${}^{T1}/_{T2} = 0.30$

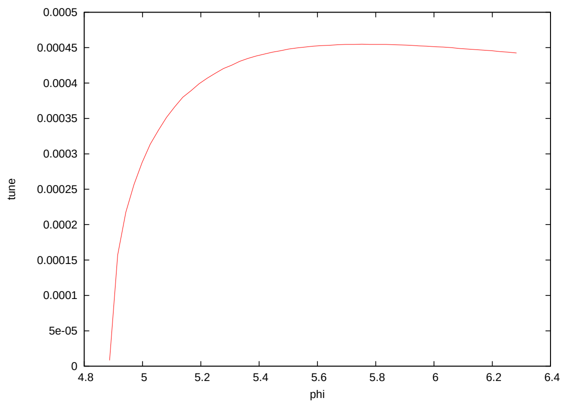

(d) ${}^{T1}/_{T2} = 0.40$

Figure 8: Plots of the the tune in the barrier rf wave for various ${}^{T1}/_{T2}$ ratios. At ${}^{1}/_{4}$ the derivative hits zero, and for a ratio above ${}^{1}/_{4}$ there is a clear maximum.

Data Analysis

Once I dumped the binary file to ascii, I then ran it through the CERN tomography code [1]. This took quite a bit of manipulation to get the program to run. With a small enough sample size and correct input flags, however, it worked without problems and reconstructed the phase space in the Main Injector.

Plotting

Even after the main tomography code was done reconstructing the phase space, the setup relied on a slow and obsolete Mathematica setup to generate the phase space plots. I replaced this with my own Python program using `matplotlib`. Plots from two bunches from the Main Injector at two different times can be seen in Figure 9. These are the same two bunches whose line shapes are shown in Figure 2.

Recycler

My next project was to modify all this code to work with the Recycler and the barrier bucket rf wave which operates differently not only in the ways described above, but the tomography code does not work for a barrier bucket and was modified for the different wave shape. However due to complications with the definition of the synchronous particle and the need for a derivative of the rf (zero everywhere except for at $0, T1, T1+T2, 2T1+T2$ where it is a delta function) this is still a work in progress. Some reconstruction has (Figure 10) been completed, but the accuracy cannot be guaranteed at this point. Nonetheless, the reconstruction showed some promise in that the scale in each dimension matched the expected values and the shapes were roughly that expected. The program diagnostics, however suggested some errors in the tracking.

Vlasov Equation

The Vlasov equation is a partial differential equation that describes the evolution of phase space density given by[4]

$$\frac{\partial f}{\partial t} + \frac{\partial f}{\partial q} \cdot \frac{\partial H}{\partial p} - \frac{\partial f}{\partial p} \cdot \frac{\partial H}{\partial q} = 0$$

This equation can be used as the theoretical counterpart to the experimental data. Instead of tracking individual particles, it instead calculates the changes to a probability density function. Since, in the Recycler, most of the action occurs in the tails where there are relatively few particles, tracking particles is very expensive and noise dependent. The Vlasov equation is solved numerically and has less noise in the tails than in particle tracking methods because it tracks a function, so information is not lost in the tails or elsewhere. The code at present, however, suffers from long term stability problems as it was designed to run for a low number of turns while in the Recycler it takes $\sim 10^5$ turns for one synchrotron period. The area of the distribution tends to diverge from 1 after a sufficiently long number of turns. Plotting the phase space distribution (Figure 11) as the code progresses can help diagnose problems before they blow up.

Conclusions and Future Work

The particle tracking provided valuable insight into the synchrotron processes in the Main Injector and the Recycler. Frequency decreases as a function of radius in phase space in a sine wave and increases

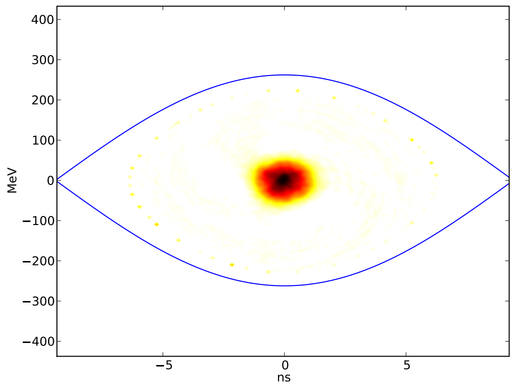

(a) At the beginning of the data set.

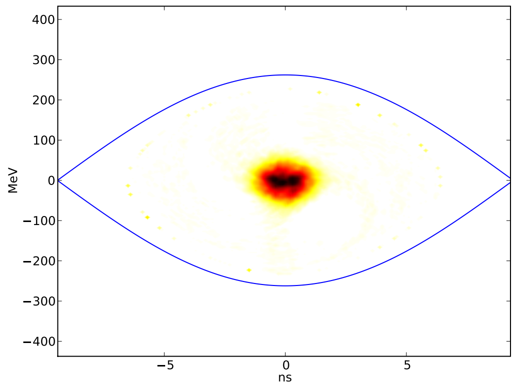

(b) At the end of the data set about twenty synchrotron periods later.

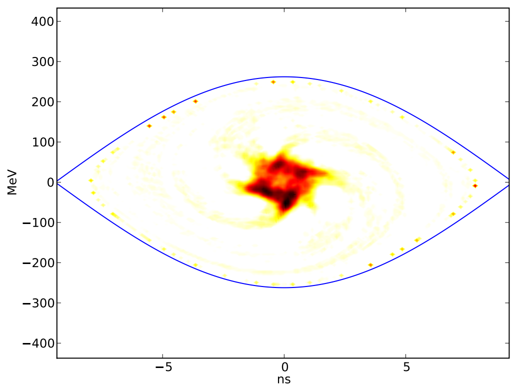

(c) A different bunch from the same data set. At the beginning of the data set.

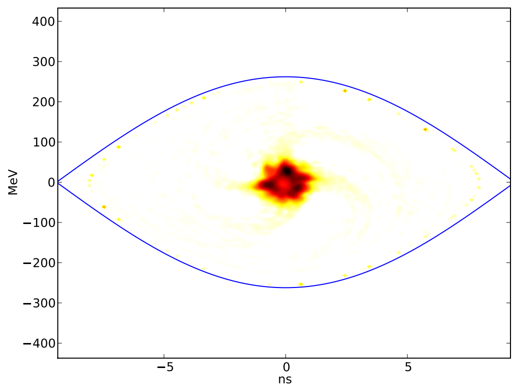

(d) At the end of the data set about twenty synchrotron periods later.

Figure 9: The phase space of two different bunches at two different times in the Main Injector. The exact times cannot, however, be identified since the line shapes over a non-zero amount of time must be used in the tomography code. Thus the result is a sort of "average." Note that different bunches can exhibit very different phase spaces.

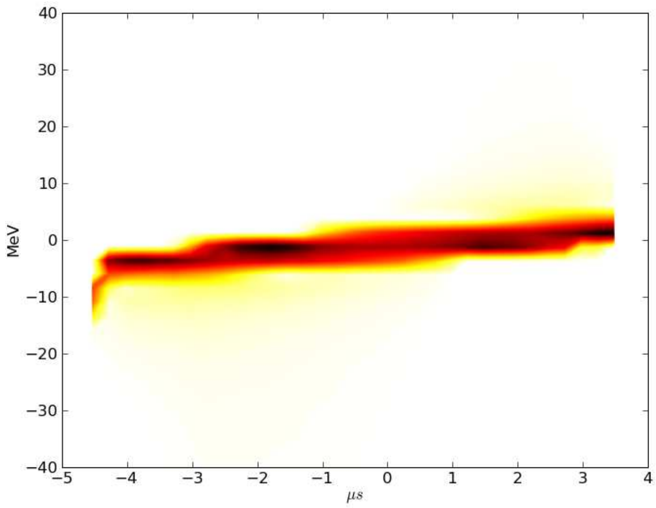

Figure 10: An attempt at the reconstruction of the phase space in the Recycler. Likely discrepancies include the slope of the bunch, the separate peaks on the left and right, and the tails going off into cut off regions.

in a barrier wave. Similarly, the tunes behave very differently. In the Main Injector there were about two synchrotron periods worth of data while in the Recycler we were limited by the scope to just under one synchrotron period, limiting the ability for accurate Recycler reconstruction. In order to run the tomography code I had to first convert the data to a usable form, then write a new graphics package, and finally understand the details of the code in order to correct for flaws in the reconstruction. Looking at the actual phase space plots, the evolution of the Main Injector phase space shows not only synchrotron rotation but also octupolar instabilities as well as sizable bunch to bunch variations. Finally, the Vlasov code will be used to compare to the experimental phase space reconstruction.

Acknowledgements

1. Tanaji Sen for his instruction and direction throughout the project.
2. The Lee Teng internship, Eric Prebys and Linda Spentzouris for organizing it.
3. Chandra Bhat for slowly walking me through the main control room operations.
4. Francois Ostiguy for explaining and installing the Vlasov code.
5. Ming-Jen Yang for walking me through the binary compression of the raw data.

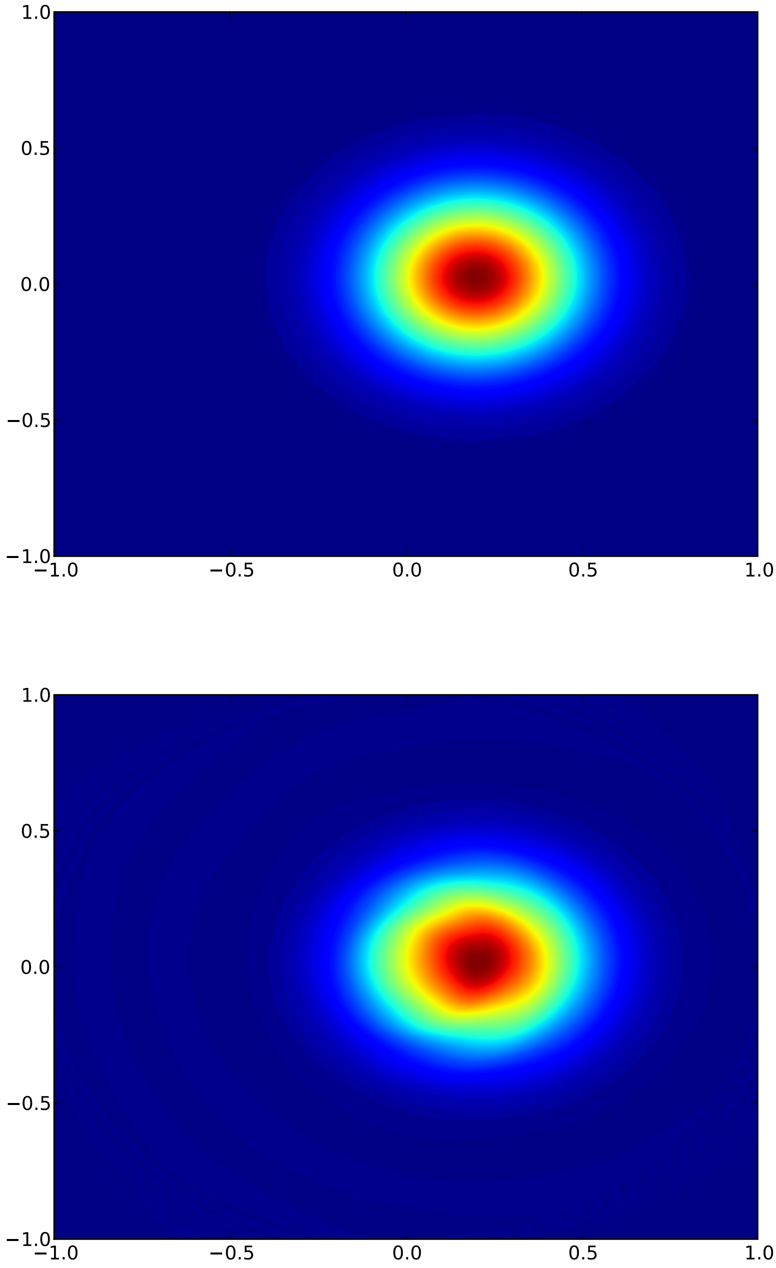

Figure 11: Given an off center bunch, it will tend to slide back towards the middle undulating as it does so.

References

[1] S. Hancock and M. Lindroos. Phase space tomography at cern. `http://tomograp.web.cern.ch/tomograp/`, April 2004.

[2] S. Y. Lee. *Accelerator Physics*. World Scientific, second edition, 2004.

[3] William H. Press, Saul A. Teukolsky, William T. Vetterling, and Brian P. Flannery. *Numerical Recipes in FORTRAN*. Cambridge University Press, second edition, 1992.

[4] Robert L. Warnock and James A. Ellison. A general method for propagation of the phase space distribution, with application to the sawtooth instability. *World Scientific*, 2000.